Consequences of a Modified Putative Substrate-Activation Site on Catalysis by Yeast Pyruvate Decarboxylase†

Jue Wang,‡ Ralph Golbik,§ Birgitta Seliger,§ Michael Spinka,§ Kai Tittmann,§ Gerhard Hübner,§ and Frank Jordan*,‡

Department of Chemistry and Program in Cellular and Molecular Biodynamics, Rutgers, The State University of New Jersey, Newark, New Jersey 07102, and Department of Biochemistry, Martin Luther University, Halle, Germany

Received May 2, 2000; Revised Manuscript Received September 25, 2000

ABSTRACT: Earlier, it had been proposed in the laboratories at Halle that a cysteine residue is responsible for the hysteretic substrate activation behavior of yeast pyruvate decarboxylase. More recently, this idea has received support in a series of studies from Rutgers with the identification of residue C221 as the site where substrate is bound to transmit the information to H92, to E91, to W412, and finally to the active center thiamin diphosphate. According to steady-state kinetic assays, the C221A/C222A variant is no longer subject to substrate activation yet is still a well-functioning enzyme. Several further experiments are reported on this variant: (1) The variant exhibits lag phases in the product formation progress curves, which can be attributed to a unimolecular step in the pre-steady-state stage of catalysis. (2) The rate of exchange with solvent deuterium of the thiamin diphosphate C2H atom is slowed by a factor of 2 compared to the wild-type enzyme, suggesting that the reduced activity that results from the substitutions some 20 Å from the active center is also seen in the first key step of the reaction. (3) The solvent (deuterium oxide) kinetic isotope effect was found to be inverse on V_{max}/K_m (0.62), and small but normal on V_{max} (1.26), virtually ruling out residue C221 as being responsible for the inverse effects reported for the wild-type enzyme at low substrate concentrations. The solvent kinetic isotope effects are compared to those on two related enzymes not subject to substrate activation, *Zymomonas mobilis* pyruvate decarboxylase and benzoylformate decarboxylase.

In a series of papers published from the Rutgers laboratories, evidence has been accumulating to support the thesis that substrate activation of the thiamin diphosphate-(ThDP-)[1] dependent yeast pyruvate decarboxylase (PDC, EC 4.1.1.1; for reaction see Scheme 1; for lead references see *1*−*7*) is triggered by interaction of pyruvate with residue C221 on the β domain (*8*−*14*), while ThDP is located at the interface of the γ domain of the same subunit and the α domain of a second subunit (Figure 1). These studies were motivated by earlier reports from the Halle group strongly suggesting that a cysteine residue was involved in the hysteretic activation process (*15*). The working hypothesis at Rutgers is that H92 on the α domain, across the domain divide from C221 on the β domain, is the recipient of the information from the substrate bound at C221; thereby H92 experiences a modest dislocation and this dislocation is propagated to E91, the adjacent residue. The information is transmitted to the γ domain by a hydrogen bond between the side-chain carboxylic acid group of E91 and the main-chain NH of W412, as well as numerous van der Waals contacts between the side chain of E91 and a short loop in the γ domain. This short loop, comprising residues 410−415, provides not only two of three conserved hydrogen bonds to the aminopyrimidine ring of ThDP (I415 to N3′

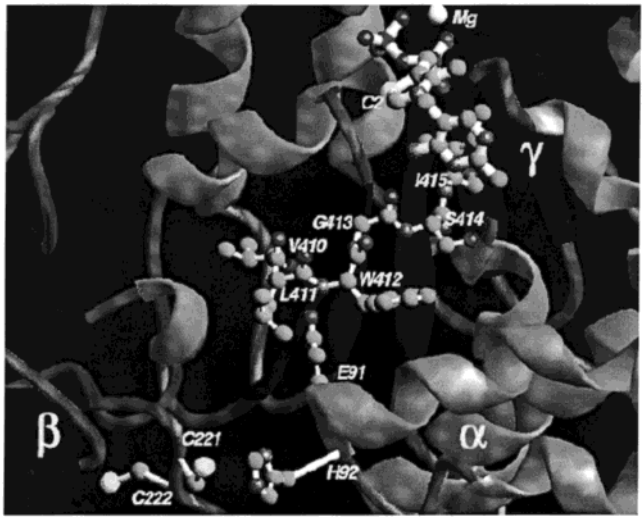

FIGURE 1: Locus of C221 and C222 with respect to the bound thiamin diphosphate (*17*).

† This work was supported at Rutgers by NIH GM-50380, the NSF Training Grant-BIR 94/13198 in Cellular and Molecular Biodynamics (F.J., PI), the Rutgers University Busch Biomedical Fund and Roche Diagnostics Corporation, Indianapolis, IN, and at Halle by the Fonds of Chemical Industrie, Germany.

* To whom correspondence should be addressed: Tel 973-353-5470; fax 973-353-1264; e-mail frjordan@newark.rutgers.edu.

‡ Rutgers, The State University of New Jersey.

§ Martin Luther University.

[1] Abbreviations: ThDP, thiamin diphosphate; PDC, pyruvate decarboxylase (EC 4.1.1.1); scpdc1, wild-type pyruvate decarboxylase isolated from *Saccharomyces cerevisiae*; WT, wild-type pyruvate decarboxylase, the yeast enzyme overexpressed in *Escherichia coli*; C221A/C222A, doubly substituted variant of this enzyme; n_H, Hill coefficient; SKIE, solvent deuterium kinetic isotope effect; ^DV, V_{max} in H_2O divided by V_{max} in D_2O at the pL plateau; $^DV/K$, ratios of the particular rate constants in water and deuterium oxide; YPDC, yeast pyruvate decarboxylase; ZmPDC, pyruvate decarboxylase from *Zymomonas mobilis.*

10.1021/bi001003r CCC: $20.00
Published on Web 01/20/2001

Scheme 1

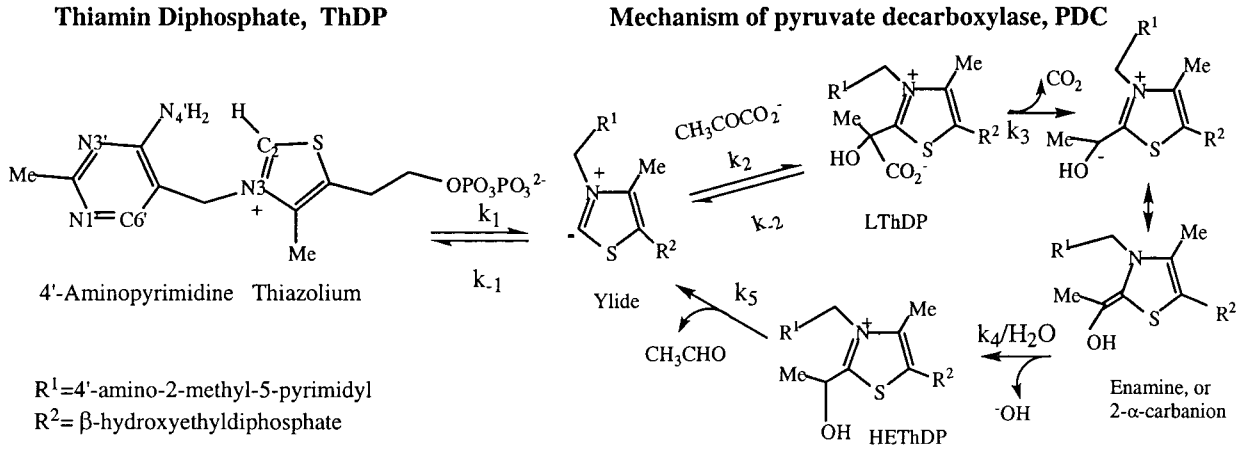

and G413 to N4′, the third one being from E51 to the N1′ atom; see refs *16* and *17*) but also the bulky hydrophobic side chain of I415, a residue whose role in supporting the V conformation and helping to create a hydrophobic environment was recently elucidated (*18*). An important consequence of the V ThDP conformation imposed by the enzyme is that the N4′ atom of the aminopyrimidine and the key C2 thiazolium atom are brought into close proximity, less than 3.2 Å from each other (*17*). So far, the combined evidence suggests that the pathway from C221 to H92 to E91 to W412 and then to G413, and ThDP provides a plausible pathway for substrate activation. Importantly, while several of the substitutions along the putative pathway reduce the Hill coefficient to near unity, i.e., abolish substrate activation, all of these substituted variants still possess significant activity.

Other aspects of our working hypothesis, used in both laboratories, include the notion that the conserved hydrogen bond between E51 and N1′ stabilizes the imino tautomeric form of the ThDP, whose N4′ imino nitrogen is basic enough and is optimally oriented by the G413 C═O to HN4′ hydrogen bond, to deprotonate the C2 atom, the first step in any ThDP-dependent reaction. The importance of this glutamic acid 51 in yeast PDC has been confirmed by substitution at this position in PDC (*7*, *19*−*22*) and was also shown at the corresponding residue in transketolase (*23*). Its involvement in the regulatory pathway appears to be complex. An additional potential participant in regulation is suggested by the X-ray structure of yeast PDC, which shows that the carbonyl oxygen of W412 forms a hydrogen bond to the imidazolyl NH atom of H115 on the α domain of a different subunit. This is one the pair of histidines (H114 and H115 in yeast PDC, H113 and H114 in ZmPDC) found to be conserved among all known PDC protein sequences from yeast, bacteria, fungi, and plants (*24*). A recent study on ZmPDC suggested that one of the two histidines, H113, is involved in substrate binding and mediates the opening and closing of the active site by ion pairing with the carboxyl group of pyruvate (*24*). Results on yeast PDC (ref *7* and manuscript in preparation) showed that the H114F but not the H115F single substitution reduces the Hill coefficient.

In this paper, the properties of the C221A/C222A variant are reexamined to provide further information about the effects of substitution at this very key site, some 20 Å from the catalytic center. This variant was selected to avoid any possible chemical intervention of C222, a residue that has been shown not to affect regulation. It is shown that the C221A/C222A variant exhibits lag phases in the progress curves for product formation (as monitored by the coupled assay with NADH and alcohol dehydrogenase), which do not result from a slow activation process but rather from a unimolecular step in the pre-steady state of the catalytic cycle. It is also shown that pyruvamide, a substrate analogue that cannot be decarboxylated but one that activates PDC (*25*), is still capable of activating the C221A/C222A variant. The data suggest that even in the absence of C221 some activation is possible, presumably since there is still the ability to bind the substrate surrogate, albeit with a much reduced binding constant. It is also shown by a technique developed in Halle (*21*) that the ThDP C2H exchange rate with solvent deuterium (examining the rate of the required first step in catalysis) is slower for the C221A/C222A variant, indicating that the C221 residue is indeed in communication with the active center coenzyme. Finally, by use of solvent deuterium kinetic isotope effect (SKIE) measurements, the transition states relating to the constants $^{D}V/K$ and ^{D}V could be compared for the C221A/C222A variant and the wild-type enzyme, as well as for the enzyme from *Zymomonas mobilis*, a PDC not subject to hysteretic substrate activation. The kinetic behavior of the C221A/C222A variant can be well described in terms of *V* and *V*/*K* since the steady-state kinetics do not give evidence for sigmoidal behavior. The results provide further evidence for the importance of C221 in the structure and mechanism of yeast PDC. Yeast PDC has also become an outstanding model for studying the details of the hysteretic substrate activation process.

EXPERIMENTAL PROCEDURES

Materials. 99.99% D_2O (glass distilled) was purchased from Isotech. Pyruvic acid sodium salt and alcohol dehydrogenase were purchased from U.S. Biochemical Corp. β-NADH was obtained from Sigma. All other materials used to make buffers were of the highest purity commercially available.

Enzyme Purification and Assay. The wild-type PDC had a His_6 tag attached to the C-terminus and was purified by use of TALON metal affinity resin from Clontech Laboratories, Inc. The enzyme was purified according to the large-scale batch purification protocol with sonication and washing buffer containing 50 mM MOPS, pH 7.5, 100 mM NaCl, 2

mM ThDP, 2 mM $MgCl_2$, and elution buffer containing 100 mM citric acid, pH 5.0, 2 mM ThDP, and 2 mM $MgCl_2$. The C221A/C222A doubly substituted variant was purified according to Farrenkopf's protocol (*26*). The crude extract supernatant after sonication was treated with ammonium sulfate to a final concentration of 2.8 M under continuous stirring at room temperature for 20 min. The pellet was collected and resuspended in 20 mM potassium phosphate buffer, pH 6.8, containing 1 mM EDTA, 2 mM $MgSO_4$, 0.5 mM phenylmethanesulfonyl fluoride (PMSF), and 0.5 mM ThDP. After dialysis in the same buffer at 4 °C overnight, the sample was purified on a DEAE-Sephacel column. Fractions containing the highest specific activity were pooled and concentrated. The enzyme activity was assayed by monitoring the aldehyde dehydrogenase-coupled depletion of NADH with time at 340 nm (*26*), and the protein concentration was determined with the Bio-Rad protein assay dye reagent (Bradford method). One unit of PDC activity is defined as the amount of enzyme required to convert 1 μmol of pyruvate to acetaldehyde per minute at 25 °C at pH 6.0. Typical specific activities (units per milligram) were 45−50 for wild type and 5−15 for the C221A/C222A variant.

Determination of the Pre-Steady-State Kinetic Parameters. Rapid reaction experiments were carried out with an Applied Photophysics SX18 MV stopped-flow spectrophotometer (Cambridge, U.K.). Pyruvate decarboxylase variant C221A/C222A (0.1−0.4 mg/mL final concentration) was mixed in a 1:1 mixing ratio with varied concentrations of sodium pyruvate (see figure captions), 328 units/mL alcohol dehydrogenase, and 0.36 mM NADH (final concentrations) either in 0.1 M PIPES buffer (pH 6.6) containing 10 mM ThDP and 10 mM $MgSO_4$ or in 0.1 M MES buffer (pH 6.0) containing 1 mM ThDP and 1 mM $MgSO_4$ at 20 °C. The decrease in NADH absorbance was observed at 340 or 366 nm. The optical path length was 10 mm. A total of 2000 data points were collected for each experiment (20 s) and 1000 points for the lag phase (0−5 s). The kinetic traces obtained with the stopped-flow spectrophotometer were fitted according to eq 1 including a single-exponential and a linear term (*25*):

$$A(t) = A_0 - \Delta A_c t - \frac{\Delta A_c}{k_{obs}} \exp(-k_{obs} t) \qquad (1)$$

where $A(t)$ is the absorbance at time t, A_0 is the extrapolated initial absorbance, ΔA_c is the constant slope after pre-steady state is achieved, and k_{obs} is the rate constant for the pre-steady-state process, respectively.

Determination of the H/D Exchange Rate at C2 of ThDP. The kinetics of H/D exchange at C2 of ThDP bound to PDC variant C221A/C222A was measured by ^{1}H NMR as described (*21*). The exchange reactions were initiated by mixing equal volumes of a sample solution containing (a) 9 mg/mL PDC variant or (b) 9 mg/mL PDC variant in the presence of 83 or 200 mM substrate analogue pyruvamide in 0.1 M sodium phosphate buffer (pH 6.0) with D_2O in a rapid quenched-flow apparatus (RQF 3, Kin Tek, Althouse) at 5 °C. Experiments with exchange times t > 2000 ms were performed by manual mixing in a thermostated reaction tube. The exchange reactions were stopped by the addition of a final concentration of 5% trichloroacetic acid and 0.1 M hydrochloric acid. After separation of the denatured protein by centrifugation, the ^{1}H NMR spectrum of the supernatant containing 2-L-ThDP was recorded in a 5 mm tube on a Bruker ARX 500 MHz NMR spectrometer. To obtain the exchange rate, the relative decay in integral intensity of the C2H signal at 9.68 ppm was fitted to a pseudo-first-order reaction. The signal of the C6′H at 8.01 ppm was used as a nonexchanging internal standard. Chemical shifts are referenced to internal 4,4-dimethyl-4-silapentane-1-sulfonic acid sodium salt (DSS) at 0 ppm.

Solvent Kinetic Isotope Effect Studies. The steady-state kinetic experiments were performed on a Cobas-Bio analyzer (Roche Diagnostic Systems) with the Holzer assay (*26*) at 25 °C. The buffers were prepared in pure H_2O and 99.99% D_2O, respectively, with the same components of MES (50 mM), MOPS (50 mM), ThDP (1 mM), $MgCl_2$ (2 mM), EDTA (0.2 mM), and NaN_3 (0.01%) and in a pL series of 5.6, 5.8, 6.0, 6.2, 6.4, 6.7, and 7.0 (assuming pD = meter reading + 0.40). For the C221A/C222A variant, the buffer components were the same except for the 50 mM MOPS, and the pL series used was from 5.6 to 6.4. Pyruvate solutions at concentrations of 0.05−65 mM were also prepared in H_2O and in D_2O. Because of the fixed diluent volume of 20 μL of H_2O after initiation of the reaction in the Cobas Bio analyzer, the percentage of deuterium oxide in the kinetics experiment is about 95%. The reactions were initiated by adding PDC enzymes to all other components.

Determination of the Steady-State Kinetic Parameters. Since the C221A/C222A variant exhibits no cooperativity (Hill coefficient is near 1.0), the steady-state kinetic data were fit to eq 2 by the SigmaPlot, Deltagraph 4.0, or KaleidaGraph 3.0 programs with nonlinear least-squares fit:

$$v_0 = \frac{VS}{K + S(1 + S/K_i)} \qquad (2)$$

The $(1 + S/K_i)$ factor accounts for the substrate inhibition observed at high pyruvate concentration, where K_i is the inhibitor dissociation constant. Plots of V and V/K for the C221A/C222A variant in both HOH and DOD were fitted and plotted against pL, from which the SKIEs were deduced.

RESULTS

Pre-Steady-State Kinetics of the C221A/C222A Variant PDC. The pre-steady-state kinetics of the C221A/C222A variant was investigated at pH 6.6 and, in some control experiments, at pH 6.0. As shown in Figure 2, the variant clearly exhibits a lag phase when product formation was detected in the coupled optical assay (*26*). To make certain that the observations concerning the lag phase monitored the rate of the PDC reaction rather than that of the ADH reaction, several controls were carried out: (i) The lag time was found to be independent of the concentration of the auxiliary enzyme alcohol dehydrogenase. The specific activity of the ADH was measured in the direction relevant to this study (acetaldehyde + NADH → ethanol + NAD^+) as 1500 units/mg at 30 °C and ample units were used in comparison with units of PDC. (ii) No lag phases were found with ZmPDC under the same assay conditions used with YPDC even with specific activity of ZmPDC of 120 units/mg (k_{cat} = 120 s^{-1}). The pyruvate concentration dependence of the rate constant characterizing the pre-steady-state at pH 6.6 is shown in Figure 3 for both wild-type (○) and C221A/C222A variant

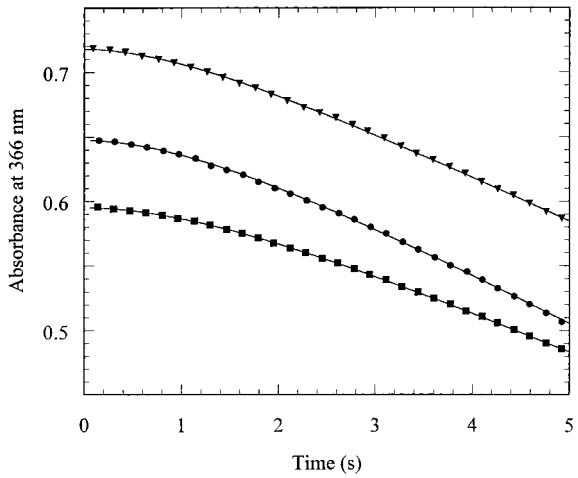

FIGURE 2: Pre-steady-state kinetics of the PDC C221A/C222A variant at 20 °C. The progress curves shown were measured in 0.1 M PIPES buffer (pH 6.6) containing 10 mM ThDP, 10 mM $MgSO_4$, and pyruvate concentrations of 20 mM (■), 50 mM (●), and 100 mM (▼). The protein concentration was 0.1 mg/mL. The curves were fitted according to the mechanism of substrate activation as described by eq 1.

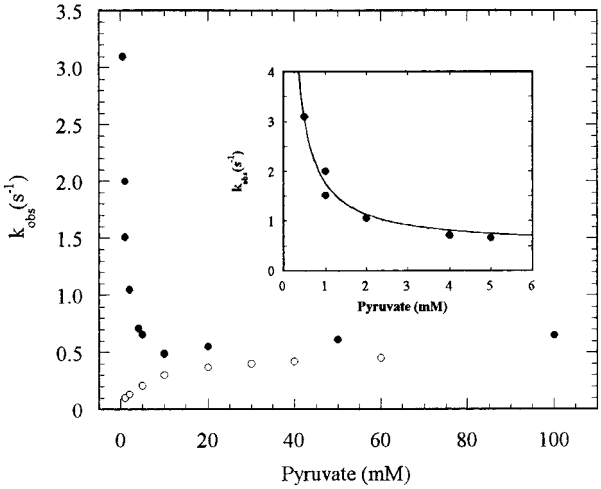

FIGURE 3: Dependence of the rate constant characterizing the pre-steady-state phase on pyruvate concentration at 20 °C for both wild-type (○) and C221A/C222A variant (●). The progress curves were measured in 0.1 M PIPES buffer (pH 6.6) containing 10 mM ThDP, 10 mM $MgSO_4$, and the indicated pyruvate concentrations. The protein concentrations ranged from 0.1 to 0.4 mg/mL. The data were fitted from 0 to 6 mM pyruvate according to eq 3. Inset: Data measured with concentrations of pyruvate to 5 mM were fitted according to eq 3, yielding a k_1 of 0.49 s^{-1}. Conditions were as described under Experimental Procedures for the coupled optical test (*26*).

(●). In contrast to the wild-type enzyme showing a hyperbolic dependence of this rate constant on substrate concentration (25), that of the C221A/C222A variant decreases with increasing substrate concentrations but reaches a constant value at substrate concentrations above 2 mM. The rate constant determined from the pre-steady state at pH 6.0 (1.5 s^{-1}) differs from that determined at pH 6.6 under comparable conditions (20 mM pyruvate) by a factor of about 2. The different concentration dependencies of the lag phases of the two enzyme forms provide strong evidence that different steps in the mechanism are being monitored.

The influence of the activator pyruvamide on the pre-steady-state kinetics of the C221A/C222A variant is demonstrated in Figure 4. The variant enzyme was preincubated

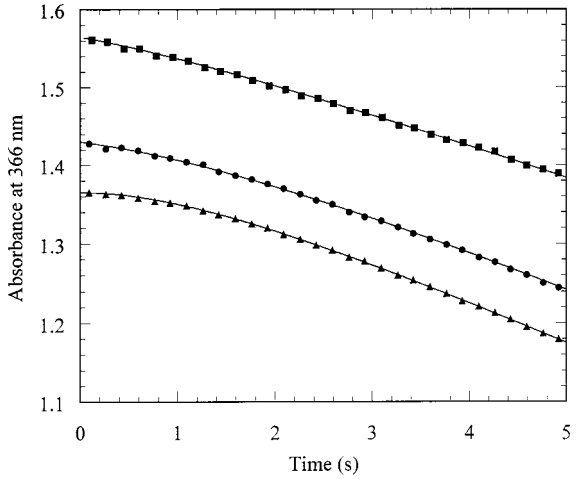

FIGURE 4: Effect of pyruvamide on the pre-steady-state kinetics of the C221A/C222A PDC variant at 20 °C. The progress curves shown were measured in 0.1 M PIPES buffer (pH 6.6) containing 10 mM ThDP and 10 mM $MgSO_4$, at 50 mM pyruvate (▲), at 50 mM pyruvate and 100 mM pyruvamide (●), and at 50 mM pyruvate and 200 mM pyruvamide (■). The protein concentration was 0.1 mg/mL.

Table 1: Exchange Rates at C2H of ThDP at 4 °C in 0.1 M Sodium Phosphate Buffer, pH 6.0, and Their Comparison to k_{cat}

species	[pyruvamide] (mM)	$k_{H/D}$ (s^{-1})	$k_{H/D}/k_{cat}$[a]
ThDP	0	0.001	not defined
yeast PDC	0	1	0.1
yeast PDC	100	>600	>60
C221A/C222A variant	0	0.54	0.22
C221A/C222A variant	83	4	1.6
C221A/C222A variant	200	12	4.8

[a] The enzymatic activity of the wild-type and mutant enzyme was determined according to Holzer (*26*) at 4 °C as described under Experimental Procedures. The k_{cat} was 10 s^{-1} for the wild-type PDC and 2.5 s^{-1} for the C221A/C222A variant at 4 °C, respectively. These data were used throughout as reference values.

with pyruvamide for 5 min before the reaction was started by addition of pyruvate. As shown in Figure 4, the progress curves in the presence of pyruvamide also exhibit lag phases. The progress curves measured in the presence of pyruvamide exhibit an initial slope that increases with increasing concentration of pyruvamide. From the increase in activity observed in the progress curves, a rate constant of approximately 0.7 s^{-1} can be calculated, which is comparable to the corresponding rate constant calculated in the absence of pyruvamide.

The temperature dependence of the enzymatic activity was determined for both enzyme species by the coupled assay (*26*). The enzyme was 6 times more active at 30 °C than at 4 °C. This factor was used in the consideration of k_{cat} and H/D exchange rate constants ($k_{H/D}$) as shown in Table 1.

To investigate whether the lag phases of the wild-type enzyme and the C221A/C222A variant PDC could be attributed to the same reaction step(s), the temperature dependence of the rate constants derived from the lag phases was determined. The Arrhenius plots for the two enzyme species (Figure 5) suggest a significantly higher activation energy for the C221A/C222A variant (120 kJ/mol) than for the wild-type PDC (75 kJ/mol).

H/D Exchange at the Thiazolium C2 Position in ThDP on PDC and on the C221A/C222A Variant. The H/D

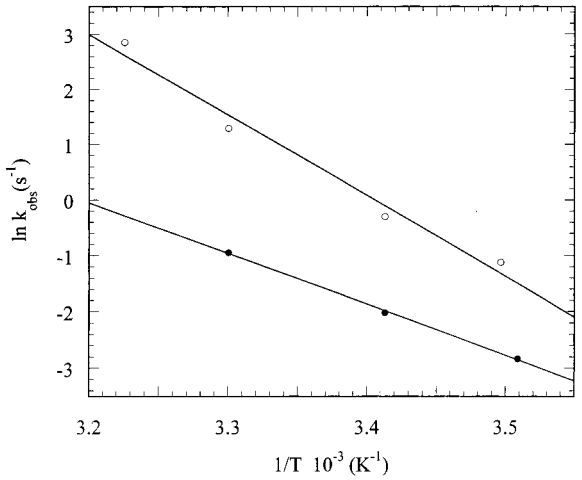

FIGURE 5: Comparison of the temperature dependence of the lag phases of wild-type (●) and C221A/C222A variant PDC (○) according to Arrhenius plots. Measurements were performed in 0.1 M PIPES buffer (pH 6.6) containing 10 mM ThDP and 10 mM $MgSO_4$, at 40 mM pyruvate for the wild type and 50 mM pyruvate for the C221A/C222A variant, respectively. The protein concentration used was 0.033 mg/mL for the wild type and 0.104 mg/mL for the C221A/C222A variant.

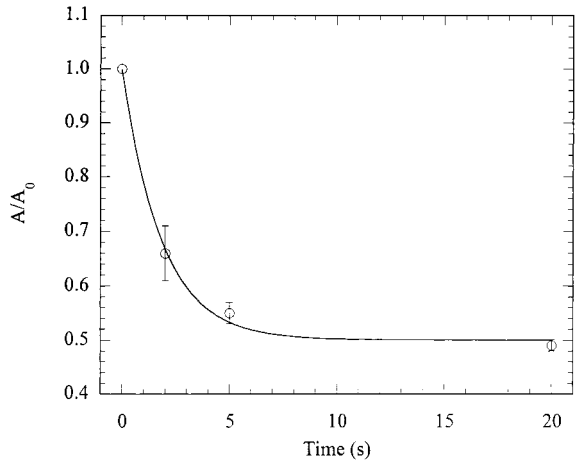

FIGURE 6: Kinetics of H/D exchange of the thiamin diphosphate C2H in the C221A/C222A PDC variant in the absence of the pyruvamide activator at 5 °C. The line represents a fit of the decay in integral intensity of the C2H signal to a single-exponential first-order reaction with $k = 0.54$ s^{-1}.

exchange rates at the thiazolium C2 position of the enzyme-bound ThDP, as well as of the free ThDP, were determined by measuring the time-dependent decay of the C2H signal (9.68 ppm) resulting from rapid mixing with D_2O, followed by acid quench. The area of the C6′H resonance (8.01 ppm) was used as a nonexchanging internal standard for quantification. As demonstrated for the C221A/C222A variant, the time-dependent decay in the integral intensity of the C2H signal can be fitted to a first-order reaction (Figure 6). In the same manner, the rate constants for H/D exchange at the C2 of ThDP in the C221A/C222A variant were determined in the absence and the presence of pyruvamide. The results (Table 1) show a decrease in H/D exchange rate at C2 of ThDP in the C221A/C222A variant in comparison with the wild-type yeast PDC. In addition, the presence of the activator pyruvamide produces different rate enhancement of the H/D exchange reaction of the C221A/C222A variant than in the wild-type PDC (Table 1). In contrast to the wild-type PDC (which experiences a dramatic H/D exchange rate acceleration by pyruvamide), in the C221A/C222A variant the exchange rate is more modestly stimulated by this activator.

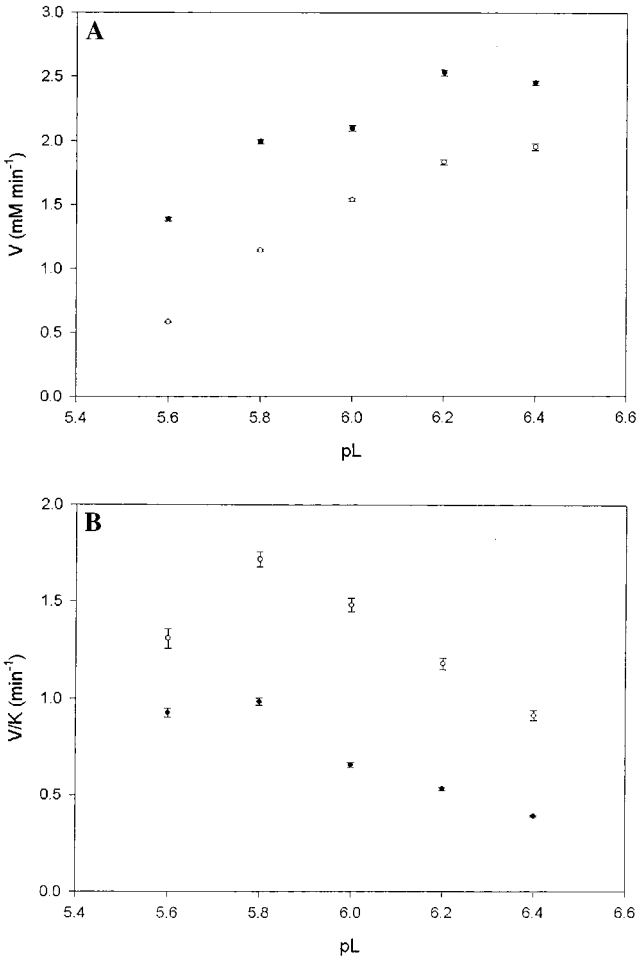

FIGURE 7: pL dependence of *V* (A) and *V*/*K* (B) for the C221A/C222A YPDC variant. (○) D_2O; (●) H_2O.

Solvent Deuterium Kinetic Isotope Effects for the C221A/C222A Variant PDC. The SKIE experiments on the C221A/C222A variant were carried out in a limited pH range. Because of the pH dependence of the steady-state kinetic parameters, it is very important to compare such values either on a plateau or at the maximum of the rate−pH profile. Importantly for this report, the C221A/C222A variant is very well behaved kinetically, i.e., it exhibits hyperbolic v_0-*S* plots, and hence the SKIE data are easier to interpret than are data obtained on the wild-type PDC, which exhibits substrate activation. In the Appendix an extended model is presented to account for the different behavior of the lag phase in product formation of wild-type and C221A/C222A variant PDCs. This model predicts a nearly hyperbolic v_0-*S* plot for small values of K_a, the dissociation constant at the regulatory site, notwithstanding the occurrence of activation processes (please see the Appendix).

pL Dependence of Steady-State Kinetic Parameters for the C221A/C222A PDC Variant. The pH(D) dependence of the steady-state kinetic parameters for the C221A/C222A variant is shown in Figure 7, with a typical data set at the same pL shown in Figure 8. In the doubly substituted variant, two of the four cysteines are absent and Michaelis−Menten kinetics are observed,;i.e., we have terms at low and high substrate

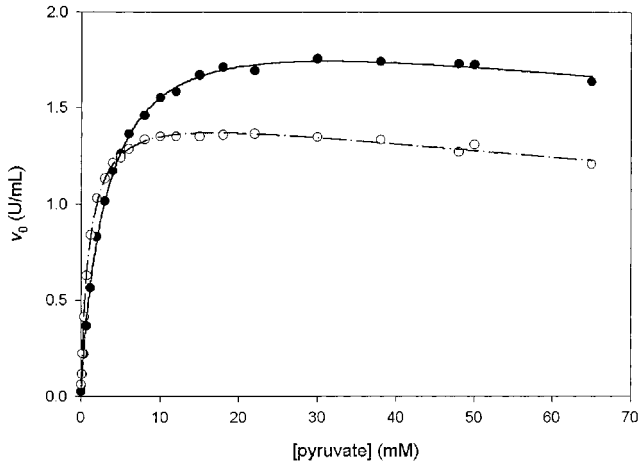

FIGURE 8: Michaelis−Menten plots for the C221A/C222A PDC variant in H_2O (●) and D_2O (○) at pL 6.0. Data were fitted to the equation $v_0 = VS/[K + S(1 + S/K_i)]$. At this pL, the fitted values of V are 2.098 ± 0.022 (H_2O) and 1.538 ± 0.012 (D_2O); the fitted values of V/K are 0.657 ± 0.012 (H_2O) and 1.483 ± 0.035 (D_2O).

Table 2: Solvent Kinetic Isotope Effects for the C221A/C222A Variant

pL	^{D}V	$^{D}V/K$
5.6	2.10 ± 0.01	0.76 ± 0.02
5.8	1.75 ± 0.01	0.57 ± 0.02
6.0	1.36 ± 0.01	0.45 ± 0.03
6.2	1.38 ± 0.02	0.45 ± 0.01
6.4	1.26 ± 0.02	0.43 ± 0.01

concentration, $^{D}V/K$ and ^{D}V. The results here reported confirm the earlier reports concerned with the C221S, C221S/C222S, C221A, and C221A/C222A variants (*9*, *11*, *12*): substrate activation is abolished by these substitutions as indicated by hyperbolic v_0-S plots. As is seen in Figure 6, V_{max} in both H_2O and D_2O increases with increasing pL, reaching a plateau near 6.0−6.4. Thus the ^{D}V values do not change much in the pL range of 5.6−6.4 and they all suggest a normal SKIE (Table 2), whether one compares them at the same pL values or at the plateaus. The SKIE at the plateau of the V_{max}–pH curve is 1.26 ± 0.02. By contrast, the pH(D)-dependent behavior of V/K exhibits an inverse isotope effect in the pL range of 5.6−6.4 for any value of pL, and $^{D}V/K$ has a value of 0.62 ± 0.03 at the plateau (Table 2).

DISCUSSION

Rate of Deprotonation at the Thiamin Diphosphate C2 Position. The results obtained from the H/D exchange rates at the ThDP C2 position indicate an approximately 2-fold slower rate for C2H ionization for the C221A/C222A variant than for the wild-type PDC. This ratio of the H/D exchange rate constants for the wild-type PDC to the C221A/C222A variant is very similar to the ratio of their specific activities (ca. 45−50 units/mg for the wild type and 15−17 units/mg for the highly purified C221A/C222A variant). This is an outstanding demonstration that substitution at C221 has a direct effect at the active center some 20 Å away; i.e., information from the C221 site can be transmitted to the catalytic center, and distortion on the β domain can be sensed at ThDP located between the α and γ domains.

Pre-Steady-State and Steady-State Kinetic Parameters. It is interesting to note that the Hill coefficient of the C221A/C222A variant was strictly unity within experimental error (ref *11* and this study). Yet, the progress curves show a lag phase in product formation (Figure 2). How can one reconcile the two sets of results? The substrate concentration dependence of the lag phase of the C221A/C222A variant is different from that of the wild-type PDC, for which the rate constant characterizing the lag phase shows hyperbolic dependence on substrate concentration. We conclude that the lag phase observed with the C221A/C222A variant should be attributed to a unimolecular step during the pre-steady-state stage of catalysis, with perhaps a small contribution from the activation process. The k_{cat} of the C221A/C222A variant is about 15 s^{-1} at 30 °C and 2.5 s^{-1} at 4 °C. Because the rate constant derived from the pre-steady state of the progress curves under saturating conditions of pyruvate is much smaller than the k_{cat} value, a unimolecular step corresponding to some conformational change of any enzyme−substrate complex cannot be responsible for the observations. A plausible alternative is that the lag phase observed with the C221A/C222A variant corresponds to the deprotonation step at C2 of ThDP, the initial reaction step in catalysis, rather than to an activation process, as observed with the wild-type enzyme. In other words, after formation of the Michaelis complex between PDC•ThDP•Mg(II) and pyruvate on the C221A/C222A variant and prior to formation of the substrate−ThDP covalent adduct 2-α-lactyl-ThDP (k_2 in Scheme 1), the thiazolium C2H must be dissociated (k_1 in Scheme 1). After decarboxylation of 2-α-lactyl-ThDP (k_3) and subsequent acetaldehyde release (k_5), the regenerated C2-carbanion of ThDP could react with the next substrate molecule without being reprotonated. According to this scenario, the observed rate constant responsible for the pre-steady-state lag phase (k_{obs}) consists of the rate constants of deprotonation (k_1) and reprotonation (k_{-1}) of the enzyme-bound ThDP C2, as well as of the on (k_2) and off rate constants (k_{-2}) for substrate binding at C2, according to

$$k_{obs} = k_1 + k_{-1}\frac{k_{-2}/k_2}{S + (k_{-2}/k_2)} \quad (3)$$

The concentration dependence of k_{obs} (Figure 3) is in agreement with this hypothesis. In addition, a comparison of the rate constant determined for the lag phase at pH 6.0, k_{obs} = 1.5 s^{-1} at 20 °C, and the rate constant for H/D exchange at C2 of the C221A/C222A variant, 0.5 s^{-1} at 4 °C, indicates that these two reactions occur on the same time scale. As shown in the Appendix, plausible models can be offered to explain the different kinetic behavior of wild-type PDC and the C221A/C222A variant.

Additional evidence for different mechanisms being responsible for the lag phases in the progress curves for product formation of the wild-type and the C221A/C222A variant PDCs is gleaned from the different activation energies determined for the two processes. From the Arrhenius plot (Figure 5), 75 kJ/mol was deduced for the wild type and 120 kJ/mol for the C221A/C222A variant. The results obtained for the C221A/C222A variant indicate that substrate activation accompanied by structural changes of the protein is not required in this substituted enzyme.

An interesting dilemma is presented in the influence of the artificial activator pyruvamide on the C221A/C222A variant: an increase in H/D exchange at C2 of the enzyme-bound ThDP and an influence on the lag phase for product

formation. Why do we see different results in the absence and presence of pyruvamide? A possible explanation is premised on the likelihood that the activator molecule at the regulatory site is held by more than a single point attachment. For example, from data of Baburina and Li (*11*, *12*) it is evident that the residue H92 is also important, both its size and charge, since Lys substitution gave a higher Hill coefficient and a more stable enzyme than Gly or Ala substitution. In addition, on the basis of model building starting with the X-ray structure, Lobell and Crout (*27*) suggested that S311 may provide two hydrogen-bond donor sites to the bound activator molecule. The crystal structure of pyruvamide-activated PDC revealed a pyruvamide binding site between the β and γ domains, about 10 Å from residue C221 (*28*, *29*). Therefore, it would not be surprising that the binding of pyruvate is different from the binding of pyruvamide and that an impaired regulatory site could still accept the activator molecule, albeit with lower affinity, as indicated by the high concentration of pyruvamide required for acceleration of H/D exchange (Table 1) as well as for reducing the lag phases (Figure 4).

We also note that the C221S substitution not only abolished (or reduced) activation but also the Hill coefficient was less than 1 (as it was for the C221S/C222S doubly substituted variant). One could argue that the serine substitution not only removes the primary binding site but can also produce additional distortion. The Cys221 to Ala substitution, on the other hand, while eliminating the key binding site, by virtue of the smaller side chain still allows the other site(s) to participate in the binding.

SKIEs on the C221A/C222A Variant. For the C221A/C222A variant, the steady-state kinetic data can be fitted throughout the pH range studied to two kinetic constants characterizing hyperbolic v_0-*S* plots both in H_2O and in D_2O, providing values of $^{D}V = 1.26$ and $^{D}V/K = 0.62$. For the C221A/C222A variant, the $^{D}V/K$ effects are inverse for all pL values, and the plateau appears to be reached near the same pL in both solvents. Also provided are the standard errors for the fit for the individual rate constants; for the ratios these errors are cumulative. On the C221A/C222A variant, the data are good enough to enable us to draw some important conclusions relative to the transition states.

The ^{D}V SKIEs are very similar for the wild-type PDC (*30*) and the C221A/C222A variant, as indeed for the ZmPDC (*31*) and even for the related enzyme benzoylformate decarboxylase ($^{D}V = 1.3$; see ref *32*). Therefore, substitution at C221 (or C222) has little or no effect on the relative energies of the transition states starting with the first irreversible step, i.e., decarboxylation, and culminating in product release. Very interestingly, the relative transition state energies starting with the decarboxylation step appear to be remarkably similar among the enzymes sharing the same function, even though ZmPDC and benzoylformate decarboxylase are not substrate-activated. Nor does benzoylformate decarboxylase (*33*) share all catalytic residues (except for structural features such as the V conformation and the three conserved hydrogen bonds around the aminopyrimidine ring) with the YPDC (*16*, *17*) and ZmPDC (*34*). However, the catalytic centers of the latter two are rather similar.

The *V*/*K* term for enzymes obeying hyperbolic kinetics offers particularly useful insight. The kinetic term *V*/*K* for the C221A/C222A variant comprises transition states resulting from the addition of pyruvate to the unactivated form of the substrate-free enzyme·ThDP·Mg(II) complex to form 2-α-lactyl-ThDP, followed by decarboxylation. The fact that to very high precision no kinetic term second-order in substrate concentration can be extracted from the kinetic data (unlike with the wild-type PDC) rules out the participation of C221 in the regulatory pathway to any significant extent once the C221A substitution is made. In assigning a role to the observed inverse SKIE on *V*/*K*, we recall the mechanism of ThDP-catalyzed decarboxylation (Scheme 1). In the absence of activation, the reaction proceeds by initial formation of a ternary substrate·PDC·ThDP complex, which is converted to the first ThDP-bound intermediate 2-α-lactyl-ThDP, that in turn undergoes decarboxylation, via the first irreversible step, hence the concluding step for *V*/*K*. It was shown some years ago at Rutgers, by use of ^{13}C kinetic isotope effects at the C1 of pyruvate (*35*) (recently confirmed on the WT PDC and also extended to the C221A/C222A variant by Chen and Huskey at Rutgers), that in this series of steps decarboxylation is only partially rate-limiting (also true of the C221A/C222A variant; Chen and Huskey, manuscript in preparation) and is faster than dissociation of 2-α-lactyl-ThDP to free reactants. It is therefore concluded that the SKIE results apply to the step in which pyruvate forms a covalent complex with the ThDP, a key step since the C2H position of ThDP must be ionized prior to, or concomitant with, this step. The simplest explanation of an inverse SKIE is that the ratio of fractionation factors for the ground state relative to that for the transition state is less than unity, implying that the hydrogen bonding is stronger in the ground state than in the transition state.

Comparison with ZmPDC and Benzoylformate Decarboxylase. Since both the wild-type ZmPDC and the YPDC C221A/C222A variant exhibit hyperbolic v_0-*S* plots, they can be compared to each other more easily than can the wild-type YPDC to its C221A/C222A variant. In fact, the SKIEs on $^{D}V/K$ are dramatically different for the two enzymes: 1.25 for ZmPDC and 0.62 for the C221A/C222A YPDC variant. A plausible explanation is that the $^{D}V/K$ obtained for ZmPDC reports on what is in essence substrate addition to an activated enzyme (for H/D exchange at C2 of ThDP, $k = 110\ s^{-1}$; see ref *21*), and the $^{D}V/K$ value for the YPDC C221A/C222A variant reports on substrate addition to an unactivated form of the enzyme (for H/D exchange at C2 of ThDP, $k = 0.5\ s^{-1}$; see Table 1). Furthermore, the fractionation factor is <1.0 for the unactivated and >1.0 for the activated enzyme conformation. Carrying this analysis over to the more complex wild-type YPDC, the suggestion is that conversion of the free enzyme to the substrate-activated state is accompanied by a major change in hydrogen bonding, namely, loosening of hydrogen bonds. At the same time, it is also useful to compare the values with that obtained on benzoylformate decarboxylase ($^{D}V/K = 1.5$; see ref *32*), similar to that obtained on ZmPDC. This comparison further suggests that the transition state resulting from addition of pyruvate (or benzoylformate) to ThDP, after or concomitant with ionization at C2 of ThDP, is the one reported by the values of $^{D}V/K$ SKIEs in both ZmPDC and benzoylformate decarboxylase.

It is also relevant to point out that, in a recent report on the C221-substituted YPDCs (*11*), the substitution was found to increase K_m while reducing the Hill coefficient from 2.0

to 1.0. In several other examples in the same paper, a Hill coefficient reduction to 1.0 led to a better (smaller) K_m. We conclude from these data that there are two distinct pathways at work, one for the C221A/C222A variant representing the unactivated form of the enzyme and the other for the enzyme capable of being activated or existing in the activated form. Examples of the latter form include the wild-type yeast PDC and ZmPDC and, based on the magnitude of $^{D}V/K$, perhaps benzoylformate decarboxylase as well.

It is also important to recall that this addition of pyruvate or benzoylformate to enzyme-bound ThDP is itself a complicated event, probably with several proton transfers, such as (for PDC) E51 to N1′, C2H to N4′, and N4′ to the carbonyl oxygen of the substrate, in addition to a variety of hydrogen bonds undergoing changes.

We finally note that the site-directed mutagenesis studies lead to assignment of observed SKIEs to specific steps in the mechanism, and, most importantly, can differentiate among mechanistic alternatives. The results obtained with the C221S and C221A variants, such as the low pK_a of the cysteine (below 6 and likely about 5.2; see ref *11*) according to both isoelectric focusing and FT-IR experiments (*10*), and especially the SKIEs here reported, rule out attribution of the inverse SKIE observed with wild-type YPDC at low pyruvate concentration to the formation of an adduct (covalent or noncovalent) between C221 and pyruvate (*30*).

APPENDIX

General Remarks. In principle, the observed lag phases in product release can be accounted for with the following mechanistic models (the specific rate constants do not necessarily correspond to those in Scheme 1):

Case A

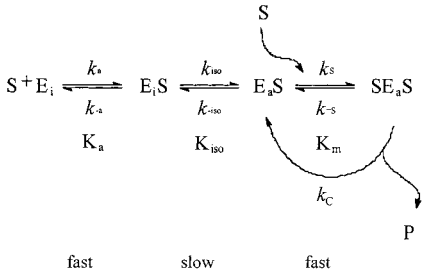

Case B

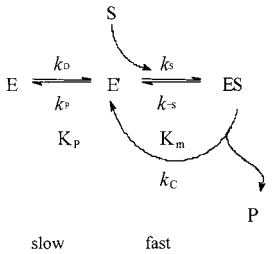

Case A describes a slow transition model involving two separate substrate binding sites and predicts sigmoidal v_0-S behavior as observed with the wild-type PDC. In case B, some pre-steady-state process (or processes), perhaps involving H/D exchange at the C2 position of ThDP, is assumed to be rate-limiting. The mechanism predicts hyperbolic v_0-S behavior, as observed with the C221A/C222A variant of PDC. Use of the following definitions

$$K_a = \frac{k_{-a}}{k_a}$$

$$K_{iso} = \frac{k_{-iso}}{k_{iso}}$$

$$K_m = \frac{k_{-S} + k_c}{k_S}$$

$$K_P = \frac{k_P}{k_D} \tag{4}$$

leads to

$$v = \frac{V_{max}S^2}{K_aK_{iso}K_m + K_m(1 + K_{iso})S + S^2} \tag{5a}$$

$$v = \frac{V_{max}S}{K_m(1 + K_P) + S} \tag{5b}$$

In each case, only one reversible step in the sequence is assumed to be slow, consistent with the essentially monophasic progress curves observed. The observed rate constant displays a typical dependence on the substrate concentration.

Derivation of the k_{obs}-S Dependencies: Case A. The relevant differential equations are the following:

$$\frac{dE_i}{dt} = -k_aE_iS + k_{-a}E_iS \tag{6}$$

$$\frac{dE_iS}{dt} = k_aE_iS - (k_{-a} + k_{iso})E_iS + k_{-iso}E_aS \tag{7}$$

$$\frac{dE_aS}{dt} = k_{iso}E_iS - (k_{-iso} + k_sS)E_aS + (k_{-S} + k_C)SE_aS \tag{8}$$

$$\frac{dSE_aS}{dt} = k_SSE_aS - (k_{-S} + k_C)SE_aS \tag{9}$$

Adding eqs 6 and 7 leads to

$$\frac{dE_i}{dt} + \frac{dE_iS}{dt} = -k_{iso}E_iS + k_{-iso}E_aS \tag{10}$$

Assuming the substrate-binding steps to be fast, the mass balance equation for all of the enzyme species reads as

$$E_0 = E_i + E_iS + E_aS + SE_aS$$
$$= E_i\left(1 + \frac{S}{K_a}\right) + E_aS\left(1 + \frac{S}{K_m}\right) \tag{11}$$

Substituting E_aS from eq 11 as well as $E_iS = E_iS/K_a$ into eq 10, after rearrangement, results in

$$\frac{dE_i}{dt} = -\left(\frac{k_{iso}S}{K_a + S} + \frac{k_{iso}K_m}{K_m + S}\right)E_i + \frac{k_{iso}E_0}{\left(1 + \frac{S}{K_m}\right)\left(1 + \frac{S}{K_a}\right)} \tag{12}$$

Thus, the k_{obs} value is described by

$$k_{obs} = \frac{k_{iso}S}{K_a + S} + \frac{k_{-iso}K_m}{K_m + S} \quad (13)$$

Case B. The relevant differential equations are the following:

$$\frac{dE}{dt} = -k_D E + k_P E' \quad (14)$$

$$\frac{dE'}{dt} = k_D E - (k_P + k_S S)E' + (k_S + k_C)ES \quad (15)$$

$$\frac{dES}{dt} = k_S S E' - (k_{-S} + k_C)ES \quad (16)$$

Here, the constants k_D and k_P may refer to the deprotonation and reprotonation at the C2 atom, respectively. Assuming fast establishment of the steady state within the catalytic cycle leads to

$$E_0 = E + E'\left(1 + \frac{S}{K_m}\right) \quad (17)$$

Following the same procedure as used in case A, one obtains the following differential equation:

$$\frac{dE}{dt} = -\left(k_D + \frac{k_P K_m}{K_m + S}\right)E + \frac{k_P E_0}{1 + \frac{S}{K_m}} \quad (18)$$

Thus

$$k_{obs} = k_D + \frac{k_P K_m}{K_m + S} \quad (19)$$

Whereas the k_{obs}-S dependence of case A may theoretically result in an upward or even downward curvature, and under certain conditions possesses extrema, eq 19 will always display a downward curvature.

REFERENCES

1. Krampitz, L. O. (1969) *Annu. Rev. Biochem. 38*, 213−240.
2. Sable, H. Z., and Gubler, C. J., Eds. (1982) *Thiamin: twenty years of progress, Ann. N.Y. Acad. Sci. 378*, 7−122.
3. Kluger, R. (1987) *Chem. Rev. 87*, 863−876.
4. Schellenberger, A., and Schowen, R. L., Eds. (1988) *Thiamin Pyrophosphate Biochemistry*, Vols. 1 and 2, CRC Press, Boca Raton, FL.
5. Bisswanger, H., and Ullrich, J., Eds. (1991) *Biochemistry and Physiology of Thiamin Diphosphate Enzymes*, pp 1−453, VCH Publishers, Weinheim, Germany.
6. Bisswanger, H., and Schellenberger, A., Eds. (1996) *Biochemistry and Physiology of Thiamin Diphosphate Enzymes*, pp 1−599, A.u.C. Intemann, Wissenschaftlicher Verlag, Prien, Germany.
7. Jordan, F., Nemeria, N., Guo, F., Baburina, I., Gao, Y., Kahyaoglu, A., Li, H., Wang, J., Yi, J., Guest, J., and Furey, W. (1998) *Biochim. Biophys. Acta 1385*, 287−306.
8. Zeng, X., Farrenkopf, B., Hohmann, S., Dyda, F., Furey, W., and Jordan, F. (1993) *Biochemistry 32*, 2704−2709.
9. Baburina, I., Gao, Y., Hu, Z., Jordan, F., Hohmann, S., and Furey, W. (1994) *Biochemistry 33*, 5630−5635.
10. Baburina, I., Moore, D. J., Volkov, A., Kahyaoglu, A., Jordan, F., and Mendselsohn, R. (1996) *Biochemistry 35*, 10249−10255.
11. Baburina, I., Li, H., Bennion, B., Furey, W., and Jordan, F. (1998) *Biochemistry*. *37*, 1235−1244.
12. Baburina, I., Dikdan, G., Guo, F., Tous, G. I., Root, B., and Jordan, F. (1998) *Biochemistry 37*, 1245−1255.
13. Li, H., Furey, W., and Jordan, F. (1999) *Biochemistry 38*, 9992−10003.
14. Li, H., and Jordan, F. (1999) *Biochemistry 38*, 10004−10012.
15. Hübner, G., König, S., and Schellenberger, A. (1988) *Biomed. Biochim. Acta 47*, 9−18.
16. Dyda, F., Furey, W., Swaminathan, S., Sax, M., Farrenkopf, B., and Jordan, F. (1993) *Biochemistry 32*, 6165−6170.
17. Arjunan, D., Umland, T., Dyda, F., Swaminathan, S., Furey, W., Sax, M., Farrenkopf, B., Gao, Y., Zhang, D., and Jordan, F. (1996) *J. Mol. Biol. 256*, 590−600.
18. Guo, F., Zhang, D., Kahyaoglu, A., Farid, R. S., and Jordan, F. (1998) *Biochemistry 37*, 13379−13391.
19. Jordan, F., Baburina, I., Gao, Y., Guo, F., Kahyaoglu, A., Nemeria, N., Volkov, A., Yi, J., Zhang, D., Machado, R., Guest, J., Furey, W., and Hohmann, S. (1996) in *Biochemistry and Physiology of Thiamin Diphosphate Enzymes* (Bisswanger, H., and Schellenberger, A., Eds.) pp 53−69, A.u.C. Intemann, Wissenschaftlicher Verlag, Prien, Germany.
20. Killenberg-Jabs, M., König, S., Eberhardt, I., Hohmann, S., and Hübner, G. (1997) *Biochemistry 36*, 1900−1905.
21. Kern, D., Kern, G., Neef, H., Tittmann, K., Killenberg-Jabs, M., Wikner, C., Schneider, G., and Hübner, G. (1997) *Science 275*, 67−70.
22. Gao, Yuhong (2000) Ph.D. Dissertation, Rutgers University, Newark, NJ.
23. Wikner, C., Meshalkina, L., Nilsson, U., Nikkola, M., Lindqvist, Y., and Schneider, G. (1994) *J. Biol. Chem. 269*, 32144−32150.
24. Schenk, G., Leeper, F. J., England, R., Nixon, P. F., and Duggleby, R. G. (1997) *Eur. J. Biochem. 248*, 63−71.
25. Hübner, G., Weidhase, R., and Schellenberger, A. (1978) *Eur. J. Biochem. 92*, 175−181.
26. Holzer, H., Schultz, G., Villar-Palasi, C. and Jutgen-Sell, J. (1956) *Biochem. Z. 327*, 331−344.
27. Lobell, M., and Crout, D. H. G. (1996) *J. Am. Chem. Soc. 118*, 1867−1873.
28. Lu, G., Dobritzsch, D., König, S., and Schneider, G. (1997) *FEBS Lett. 403*, 249−253.
29. Lu, G., Dobritzsch, D., Baumann, S., Schneider, G. and König, S. (2000) *Eur. J. Biochem. 267*, 861−868.
30. Alvarez, F. J., Ermer, J., Hübner, G., Schellenberger, A., and Schowen, R. L. (1995) *J. Am. Chem. Soc. 117*, 1678−1683.
31. Sun, S., Duggleby, R. G., and Schowen, R. L. (1995) *J. Am. Chem. Soc. 117*, 7317−7322.
32. Weiss, P. M., Garcia, G. A., Kenyon, G. L., Cleland, W. W., and Cook, P. F. (1988) *Biochemistry 27*, 2197−2205.
33. Hasson, M. S., Muscate, A., McLeish, M. J., Polovnikova, L. S., Gerlt, J. A., Kenyon, G. L., Petsko, G. A., and Ringe, D. (1998) *Biochemistry 37*, 9918−9930.
34. Dobritzsch, D., König, S., Schneider, G., and Lu, G. (1998) *J. Biol. Chem. 273*, 20196−20204.
35. Jordan, F., Kuo, D. J., and Monse, E. U. (1978) *J. Am. Chem. Soc. 100*, 2872−2878.
36. Farrenkopf, B., and Jordan, F. (1992) *Protein Expression Purif. 3*, 101−107.

BI001003R